

UC Irvine

ICTS Publications

Title

Intravascular atherosclerotic imaging with combined fluorescence and optical coherence tomography probe based on a double-clad fiber combiner

Permalink

<https://escholarship.org/uc/item/6dt1r43k>

Journal

Journal of Biomedical Optics, 17(7)

ISSN

1560-2281

Authors

Liang, Shanshan
Saidi, Arya
Jing, Joe
et al.

Publication Date

2012-06-28

Peer reviewed

Journal of Biomedical Optics

SPIEDigitalLibrary.org/jbo

Intravascular atherosclerotic imaging with combined fluorescence and optical coherence tomography probe based on a double-clad fiber combiner

Shanshan Liang
Arya Saidi
Joe Jing
Gangjun Liu
Jiawen Li
Jun Zhang
Changsen Sun
Jagat Narula
Zhongping Chen

Intravascular atherosclerotic imaging with combined fluorescence and optical coherence tomography probe based on a double-clad fiber combiner

Shanshan Liang,^{a,b} Arya Saidi,^b Joe Jing,^b Gangjun Liu,^b Jiawen Li,^b Jun Zhang,^b Changsen Sun,^a Jagat Narula,^c and Zhongping Chen^b

^aDalian University of Technology, School of Physics and Optoelectronic Engineering, Ganjingzi District, Dalian City, Liaoning Province, China

^bUniversity of California, Irvine, Beckman Laser Institute, Irvine, California

^cUniversity of California, Division of Cardiology, Medical Center, Irvine, Orange, California

Abstract. We developed a multimodality fluorescence and optical coherence tomography probe based on a double-clad fiber (DCF) combiner. The probe is composed of a DCF combiner, grin lens, and micromotor in the distal end. An integrated swept-source optical coherence tomography and fluorescence intensity imaging system was developed based on the combined probe for the early diagnoses of atherosclerosis. This system is capable of real-time data acquisition and processing as well as image display. For fluorescence imaging, the inflammation of atherosclerosis and necrotic core formed with the annexin V-conjugated Cy5.5 were imaged. *Ex vivo* imaging of New Zealand white rabbit arteries demonstrated the capability of the combined system. © 2012 Society of Photo-Optical Instrumentation Engineers (SPIE). [DOI: 10.1117/1.JBO.17.7.070501]

Keywords: optical coherence tomography; fluorescence; atherogenesis; double-clad fiber; annexin V.

Paper 12219L received Apr. 6, 2012; revised manuscript received May 16, 2012; accepted for publication May 22, 2012; published online Jun. 28, 2012.

1 Introduction

Atherosclerosis can cause serious cardiovascular diseases. The rupture of atherosclerotic plaque can lead to embolisms downstream and the occurrence of acute coronary syndromes such as myocardial infarction and stroke, which cause irreversible damage to patients or even lead to their deaths. Therefore, early detection of plaque lesions is very important to prevent lethal consequences of atherosclerosis. Diagnosis of the latent vulnerability of a plaque lesion relies on both structural and tissue chemical compositions. Structurally, the thickness of the fibrous cap is a reliable indicator of plaque vulnerability. Chemically, the intralumen lipid density is a parameter that

correlates with the vulnerability of the lesion.¹ Intravascular ultrasound (IVUS) and optical coherence tomography (OCT), currently the two most commonly used modalities in clinics for diagnosing cardiovascular diseases, allow direct tomographic visualization of cross-sectional images from inside the vessel lumen.² IVUS has been used clinically to diagnose atherosclerosis for more than 20 years. However, IVUS has limited resolution of 50 to 200 μm , which is not enough to resolve the thin fiber cap of the high-risk vulnerable plaque with typical thicknesses of 50 to 60 μm . On the other hand, OCT can provide cross-sectional images of tissue microstructure with a spatial resolution on the order of 5 to 10 μm .³ Therefore, intravascular OCT can be used to accurately assess thickness of fibrous caps and other microstructure information of vulnerable plaques.^{4,5} Although OCT has been used for vulnerable plaque evaluation with its high resolution, it lacks molecular specificity for identification of tissue composition in plaques. Intravascular fluorescence molecular imaging endoscopy provides biomolecular information of atherosclerosis inside the blood vessel.⁶ Therefore, an integrated OCT/fluorescence imaging system^{7,8} combining high spatial resolution of OCT with molecular sensitivity of fluorescence imaging is capable of resolving both microstructure and biomolecular information at the same time.

In this paper, an integrated swept-source OCT and fluorescence intensity imaging system was demonstrated based on a multimodality endoscopic probe. A micromotor was used for circumferential scanning of the inner blood vessel wall. This distal scanning design eliminates the disadvantage of unstable vibration and uneven rotational speed in a proximal scanning design and can be applied to more flexible materials without the need of rotational torque transfer.⁹ The OCT and fluorescence imaging were obtained synchronously and in real time. The capability of the integrated OCT-fluorescence imaging system was demonstrated by *ex vivo* imaging of specimens from New Zealand white rabbit arteries.

2 Materials and Methods

The diagram of an integrated swept-source OCT (SSOCT) fluorescence system is shown in Fig. 1(a). The SSOCT system is similar to the one used in Ref. 2. A continuous-wave laser diode (Messtel, RS635) with a center wavelength of 635 nm and output power of 5 mW was used as the excitation source. A photomultiplier tube (PMT) (Hamamatsu, H9305-01) was used to detect fluorescence emission light. For our experiments, we used Cy5.5, a fluorescence dye with a peak excitation wavelength of around 675 nm (33% of the peak efficiency at 635 nm) and a peak emission wavelength of around 690 nm. The excitation light and the OCT beam were combined together with a wavelength division multiplexer (WDM coupler 635/1310). A double-clad fiber (DCF) combiner [Avensys Tech, (2 + 1) × 1 Pump and Signal Combiners, MMC02112A60] with one single-mode fiber port, one multimode fiber port, and one DCF port was used to deliver the OCT and fluorescence excitation light beams to the sample and collect the OCT signal and fluorescence emission light. The OCT signal and fluorescence excitation light were transported through the 8- μm core of the DCF, and the back-reflected fluorescence emission light was collected through the 105- μm inner cladding of the DCF. Fluorescence emission light back-scattered from the sample was coupled back through the multimode fiber port of the

Address all correspondence to: Zhongping Chen, 1002 Health Sciences Road East, Beckman Laser Institute, University of California, Irvine, California 92612. Tel: 949 824 1247; Fax: 949 824 8413; E-mail: z2chen@uci.edu

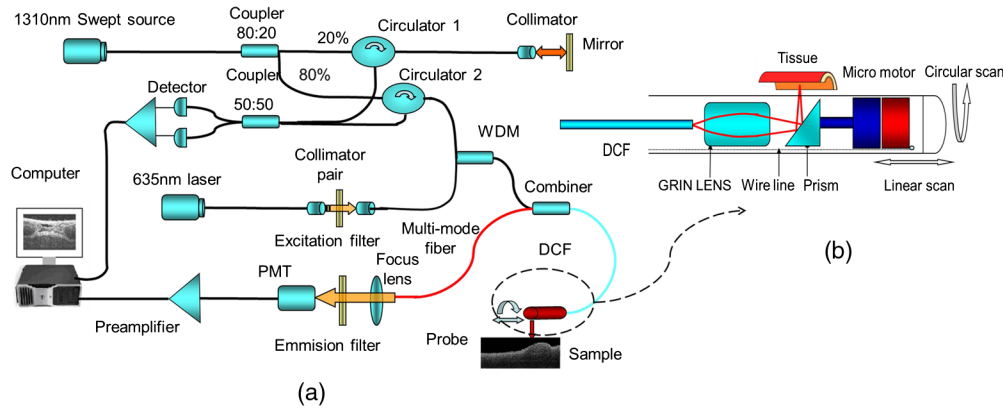


Fig. 1 (a) Schematic of the optical coherence tomography (OCT)-fluorescence system. Black line denotes single-mode fiber (SMF28), red line denotes multimode fiber, and blue line denotes double-clad fiber (DCF). (b) Intravascular probe based on a DCF combiner. OCT and fluorescence excitation light are transported through the single-mode core of the DCF; the back-reflected fluorescence emission light is collected through the inner cladding of the DCF.

combiner and detected by the PMT. The use of single-mode DCF core to deliver the fluorescence excitation light improved lateral resolution of the fluorescent image.

The diagram of the dual-modality intravascular probe with outer diameter of 2.3 mm is shown in Fig. 1(b). A linear motor outside the endoscope was used to pull back the entire probe to create 3-D helical OCT scanning and achieve a 2-D superficial fluorescence intensity image. OCT and fluorescence emission signals were digitized by a two-channel, 250 M samples/s, 12-bit data acquisition card and transferred to a

computer for processing. Data processing software was developed to handle OCT and fluorescence data acquisition, processing, image display, and data saving simultaneously and in real time.

To evaluate the integrated system, we imaged an excised segment of normal New Zealand white rabbit aorta injected with 0.01 mL of a model plaque material of highly saturated grease. Two model plaques were made side by side on the same piece of tissue, with one mixed with 0.1 $\mu\text{mol/L}$ Cy5.5. In addition, an atherosclerosis-induced New Zealand white rabbit aorta was

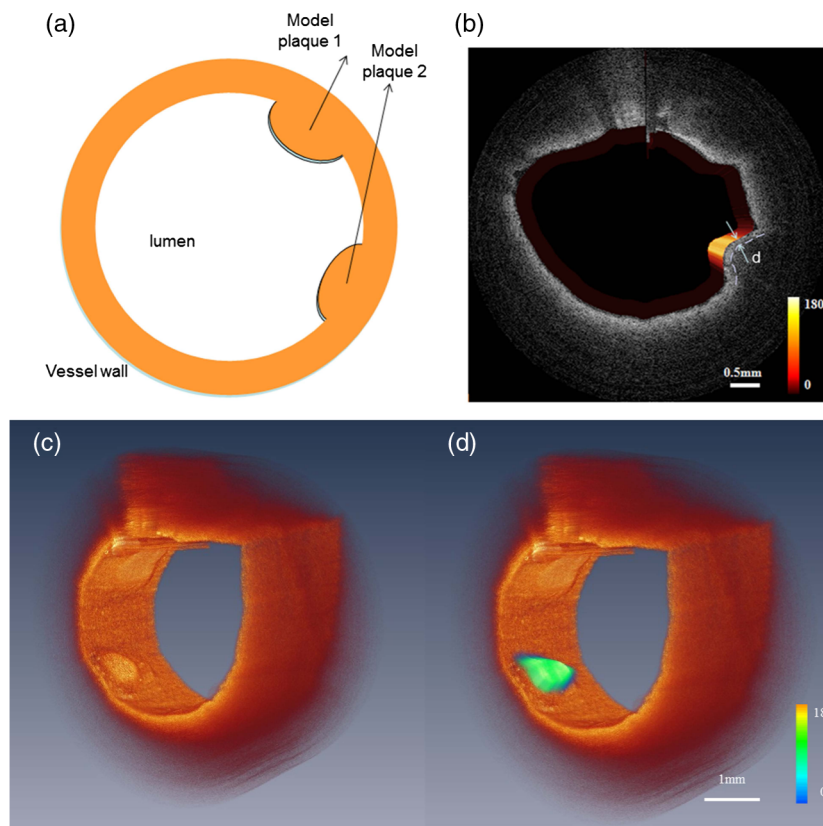


Fig. 2 Schematic (a) and fused fluorescence- optical coherence tomography (OCT) image (b) of normal rabbit aorta injected with 0.01 mL of model plaque material. The thickness of the plaque cap is around 128 μm as indicated in label (d). The color scale in (b) shows the relative intensity of the fluorescence signal. 3-D OCT image (c) is combined with 2-D fluorescence image (d).

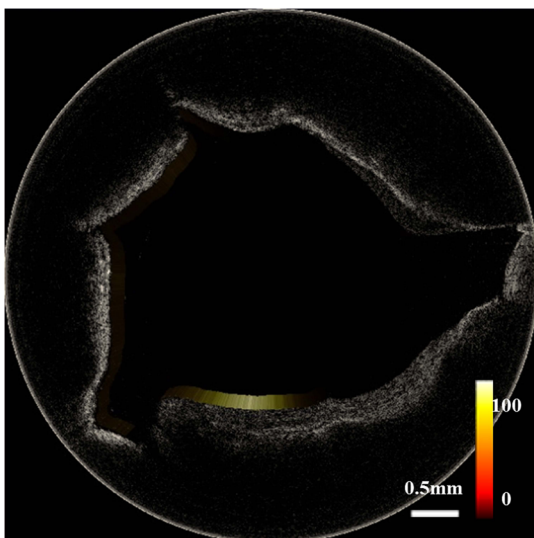


Fig. 3 Combined optical coherence tomography-fluorescence image of a stained atherosclerotic rabbit aorta specimen.

imaged for *ex vivo* study.¹⁰ Annexin V–conjugated Cy 5.5 was used to target the plaques and stain the tissue. The tissue was stained for 24 h before imaging. Annexin V is an antibody that targets apoptotic macrophages that accumulate in the necrotic core, a key feature of vulnerable plaques.¹¹

3 Results and Discussion

Figure 2(a) shows the schematic of the two phantom plaques inside the blood vessel wall. Figure 2(b) illustrates the fused fluorescence-OCT image of the model plaques. The power of OCT on the sample is around 1.5 mW. The fluorescence signal was obtained by averaging the fluorescence signal within an OCT a-line acquisition time. The fluorescence signal was generated from the model plaque under the tissue surface, demonstrating that our system is capable of detecting weak signals from deep tissue. Figure 2(c) shows the 3-D OCT image and Fig. 2(d) shows that the OCT image of the mimic plaque matches well with the 2-D fluorescence intensity image. This experiment demonstrates that our system is capable of detecting both OCT and fluorescence intensity signals simultaneously.

In addition, we carried out an *ex vivo* study on an atherosclerotic rabbit aorta, stained with annexin V–conjugated Cy5.5, which contained some plaques. Figure 3 shows the cross-sectional OCT image and the corresponding fluorescence intensity image of the sample. From the OCT image in Fig. 3, it is hard to distinguish the structural difference between all the bumps, whereas the fluorescence intensity image indicates that certain regions contain phosphatidylserine (the target for apoptotic macrophages) by detecting annexin V which was bound to it. The phosphatidylserine in these regions is due to formed necrotic cores or inflammation with significant macrophage infiltration, which are the characteristics of early-stage vulnerable plaques.

The integration of these two techniques will help to detect high-risk plaques at an earlier stage. OCT is capable of detecting structural features, such as the thickness of the plaque cap and a large lipid pool. Fluorescence intensity imaging can show the molecular information underlying the atherosclerotic plaque,

such as inflammation or the formation of a necrotic core. We can choose different agents to target various molecular factors for high-vulnerability plaques. Therefore, integrating these two modalities will provide physicians with a powerful tool to image and diagnose vulnerable plaques and monitor therapeutic efficacy at an earlier stage than is currently possible.

4 Conclusion

We present an integrated OCT and fluorescence intensity imaging system that can be used in cardiology to diagnose and detect high-risk vulnerable plaques. The system is capable of real-time OCT imaging as well as superficial fluorescence intensity imaging simultaneous. The *ex vivo* experiment showed that this integrated imaging modality can provide both structure and molecular information that may enable diagnosing vulnerable plaque at an earlier stage. Although significant research remains to be done to translate this technology to clinical applications, the results reported here clearly demonstrate the potential of integrated OCT-fluorescence imaging for characterization and diagnosis of vulnerable plaques. Furthermore, the integrated OCT-fluorescence imaging system can also be used for imaging and diagnosis of cancers in gastrointestinal, respiratory, and urogenital tracts.

Acknowledgments

This work is based on the research supported by the NIH (grants R01EB-10090, R01HL-105215, K25HL-102055, and P41-EB2182) and the AFOSR (FA9550-08-1-0384). Shanshan Liang is supported in part by the China Scholarship Council (CSC) and works as a joint Ph.D. student at the Beckman Laser Institute, University of California, Irvine.

References

1. R. P. Choudhury and E. A. Fisher, "Molecular Imaging in atherosclerosis, thrombosis, and vascular inflammation," *Arterioscler. Thromb. Vasc. Biol.* **29**(7), 983–991 (2009).
2. J. Yin et al., "Integrated intravascular optical coherence tomography ultrasound imaging system," *J. Biomed. Opt.* **15**(1), 010512 (2010).
3. W. Drexler, "Ultrahigh-resolution optical coherence tomography," *J. Biomed. Opt.* **9**(1), 47–74 (2004).
4. Y. Liu et al., "Assessment by optical coherence tomography of stent struts across side branch: comparison of bare-metal stents and drug-eluting stents," *Circ. J.* **75**(1), 106–112 (2011).
5. H. C. Yang et al., "A dual-modality probe utilizing intravascular ultrasound and optical coherence tomography for intravascular imaging applications," *IEEE Trans. Ultrason. Ferroelectr. Freq. Control* **57**(12), 2839–2843 (2010).
6. M. A. Calfon et al., "Intravascular near-infrared fluorescence molecular imaging of atherosclerosis: toward coronary arterial visualization of biologically high-risk plaques," *J. Biomed. Opt.* **15**(1), 11107 (2010).
7. H. Yoo et al., "Intra-arterial catheter for simultaneous microstructural and molecular imaging in vivo," *Nat. Med.* **17**(12), 1680–1684 (2011).
8. A. R. Tumlinson et al., "Miniature endoscope for simultaneous optical coherence tomography and laser-induced fluorescence measurement," *Appl. Opt.* **43**(1), 113–121 (2004).
9. J. Su et al., "In vivo three-dimensional microelectromechanical endoscopic swept source optical coherence tomography," *Opt. Express* **15**(16), 10390–10396 (2007).
10. K. Ohtsuki et al., "Detection of monocyte chemoattractant protein-1 receptor expression in experimental atherosclerotic lesions," *Circulation* **104**(2), 203–208 (2001).
11. P. Libby, "Inflammation in atherosclerosis," *Nature* **420**(6917), 868–874 (2002).